Coupled Ostrovsky equations for internal waves on a shear flow

Karima Khusnutdinova

Department of Mathematical Sciences, Loughborough University, UK

K.Khusnutdinova@lboro.ac.uk

Joint work with

A. Alias, R.H.J. Grimshaw, Loughborough University, UK

SCT - 2014, 4 - 8 August 2014

in honour of Vladimir Zakharov's 75th birthday

L.D. Landau Institute for Theoretical Physics
Chernogolovka, Russia

Overview

- Introduction.
- Coupled Ostrovsky equations for strongly interacting internal waves in a rotating ocean with a shear flow.
- Three-layer model with a piecewise-constant shear flow. Dispersion relations and dynamics.
- Concluding remarks.

Introduction: observations of internal waves

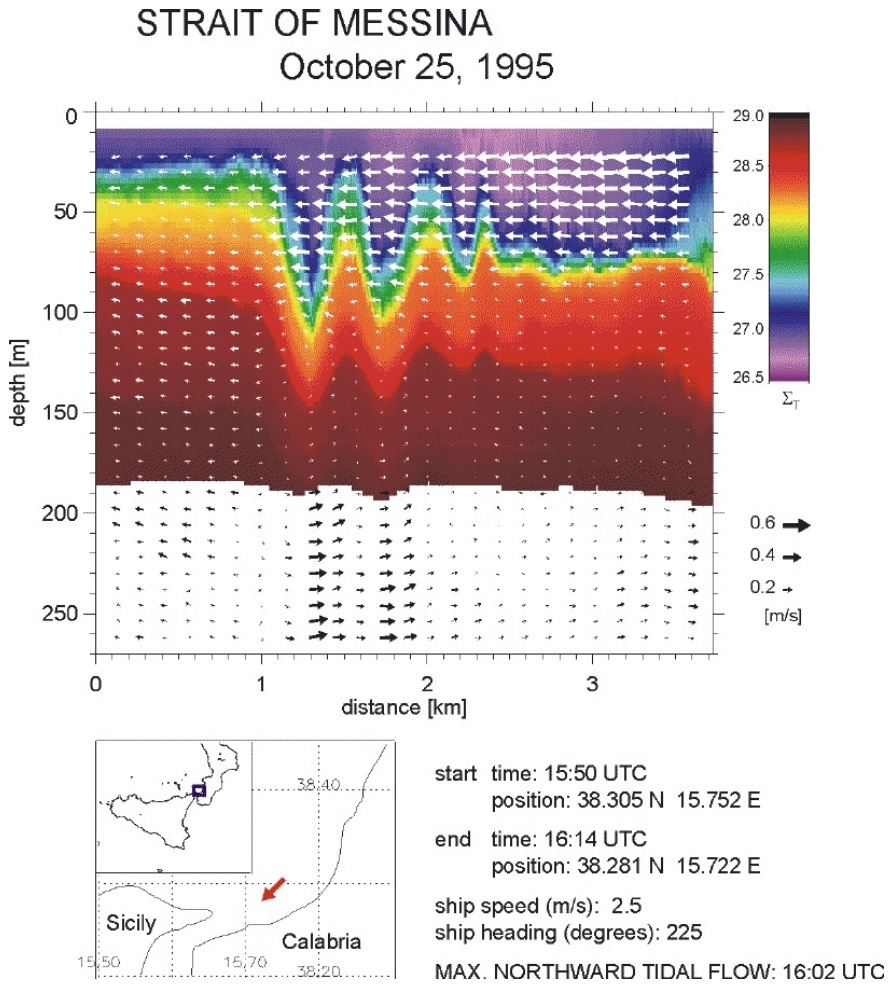

Figure: Undular bore in the Strait of Messina, *from* http://earth.esa.int/ers/instruments/sar/applications/ERS-SARtropical/oceanic/intwaves/intro/

Introduction: observations of internal waves

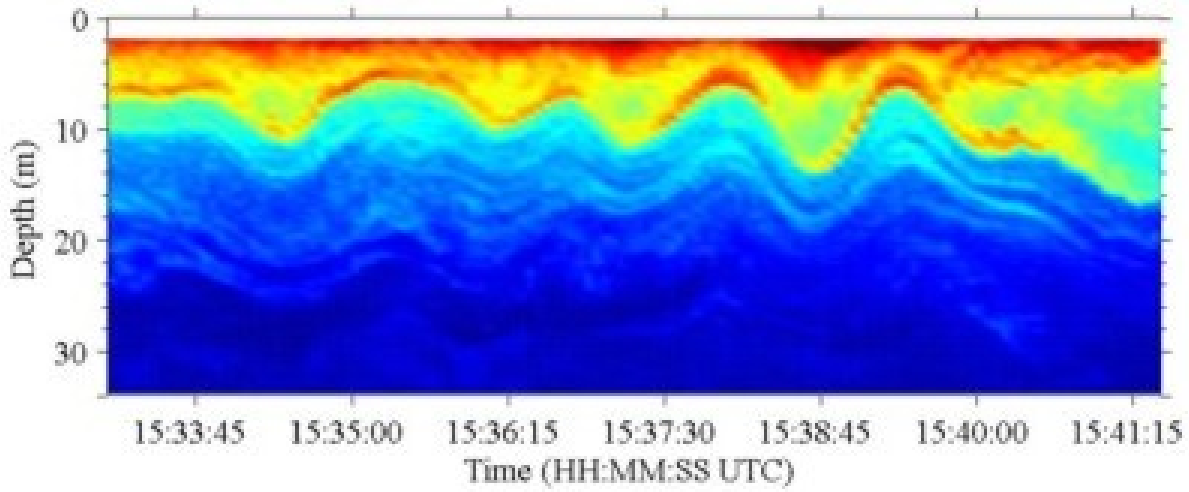

Figure: Large-amplitude internal waves in the St. Lawrence - Saguenay coastal system, *from* http://myweb.dal.ca/kelley/SLEIWEX/index.php

Introduction: effect of rotation

The evolution of weakly-nonlinear, long internal waves with rotation is described by the rotation-modified Korteweg-de Vries (KdV) equation or Ostrovsky equation (Ostrovsky 1978)

$$\{A_t + \nu A A_x + \lambda A_{xxx}\}_x = \gamma A$$

where ν and λ are the coefficients of nonlinear and dispersive terms, respectively and the parameter $\gamma = f^2/2c_0$ measures the effect of rotation when there is no shear flow. Here, c_0 is the linear long wave phase speed and f is the local Coriolis parameter.

Aim: to derive and study coupled Ostrovsky equations for the case when a system supports two different long-wave modes with nearly coincident phase speeds in the presence of a shear flow, extending the previous work on coupled KdV equations (Gear and Grimshaw 1984, Grimshaw and Iooss 2003, etc.)

Coupled Ostrovsky equations have also emerged in the context of waves in layered elastic waveguides with the soft bonding layer (Khusnutdinova and Moore 2011).

Introduction: effect of rotation

For oceanic waves (no shear flow) $\lambda\gamma > 0$, emergence of an unsteady nonlinear wave packet (Helfrich 2007, Grimshaw and Helfrich 2012).

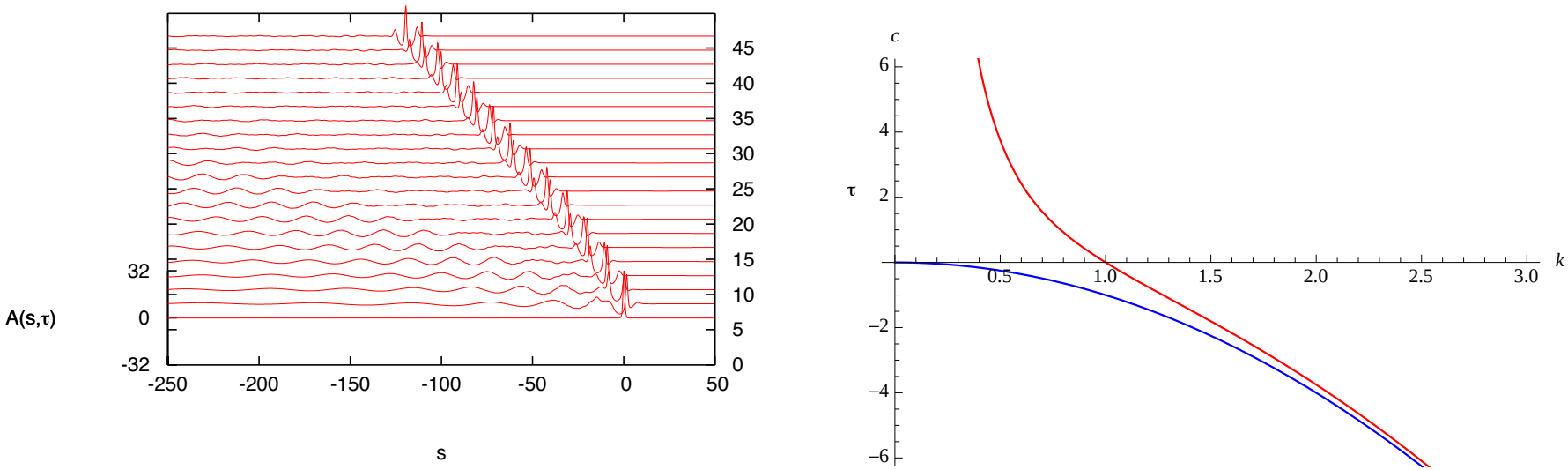

Figure: LHS: Numerical solution of the Ostrovsky equation with the KdV soliton initial condition (amplitude $A_0 = 32$ and $\nu = \lambda = \gamma = 1$). RHS: Phase velocity for KdV equation (blue curve) and Ostrovsky equation (red curve).

When $\lambda\gamma < 0$ the Ostrovsky equation can support steady envelope wave packets (Galkin and Stepanyants 1991, Obregon and Stepanyants 1998): magneto - acoustic waves in a rotating plasma.

Derivation of coupled Ostrovsky equations

We consider 2-D flow of an inviscid, incompressible fluid on a rotating f-plane. In the basic state the fluid has depth h, density stratification $\rho_0(z)$, a corresponding pressure $p_0(z)$ such that $p_{0z} = -g\rho_0$ and a horizontal shear flow $u_0(z)$ in the x-direction.

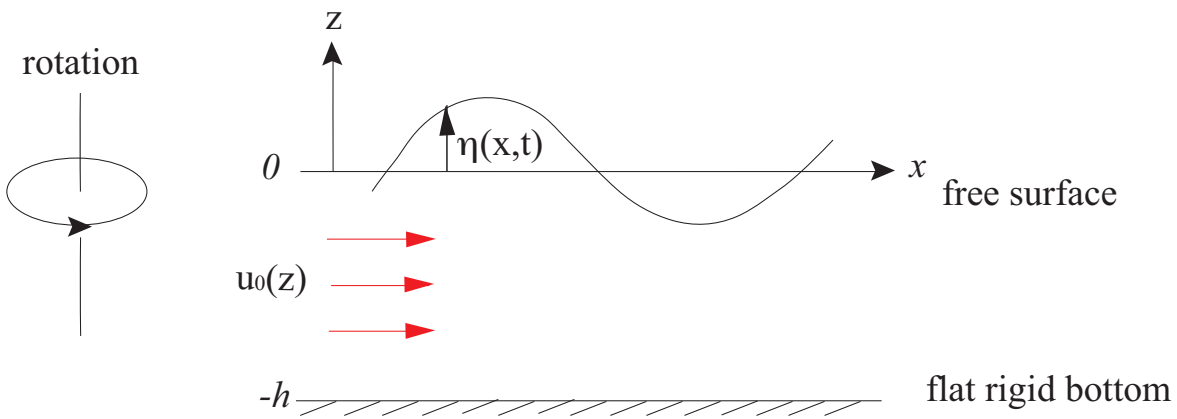

Figure: Configuration of the flow

Derivation of coupled Ostrovsky equations

Then the equations of motion relative to the basic state are,

$$\begin{aligned}
\rho_0(u_t + u_0 u_x + w u_{0z}) + p_x &= -(\rho_0 + \rho)(u u_x + w u_z - f v) - \rho(u_t + u_0 u_x + w u_{0z}), \\
\rho_0(v_t + u_0 v_x + f u) + \rho f u_0 &= -(\rho_0 + \rho)(u v_x + w v_z) - \rho(v_t + u_0 v_x) - \rho f u, \\
p_z + g\rho &= -(\rho_0 + \rho)(w_t + (u_0 + u) w_x + w w_z), \\
g(\rho_t + u_0 \rho_x) - \rho_0 N^2 w &= -g(u \rho_x + w \rho_z), \\
u_x + w_z &= 0.
\end{aligned}$$

Here, $N(z)$ is the buoyancy frequency, defined by $\rho_0 N^2 = -g\rho_{0z}$ and f is the Coriolis parameter. The free surface and rigid bottom boundary conditions to the above problem are given by

$$\begin{aligned}
p_0 + p = 0 \quad &\text{at} \quad z = \eta, \\
\eta_t + (u_0 + u)\eta_x = w \quad &\text{at} \quad z = \eta, \\
w = 0 \quad &\text{at} \quad z = -h.
\end{aligned}$$

The vertical particle displacement ζ is defined by the equation

$$\zeta_t + (u_0 + u)\zeta_x + w\zeta_z = w,$$

and satisfies the boundary condition $\zeta = \eta$ at $z = \eta$.

Derivation of coupled Ostrovsky equations

To derive coupled Ostovsky equations we introduce the scaled variables

$$\tau = \epsilon\alpha t\,, \quad \theta = \epsilon(x - ct)\,, \quad f = \alpha\tilde{f}$$

where $\alpha = \epsilon^2$ and seek a solution of the form

$$\begin{aligned} [\zeta, u, \rho, p] &= \alpha[\zeta_1, u_1, \rho_1, p_1] + \alpha^2[\zeta_2, u_2, \rho_2, p_2] + \cdots\,, \\ [w, v] &= \alpha\epsilon[w_1, v_1] + \alpha^2\epsilon[w_2, v_2] + \cdots \end{aligned}$$

At the leading order,

$$\zeta_1 = A_1(\theta, \tau)\phi_1(z) + A_2(\theta, \tau)\phi_2(z),$$

where $\phi_1(z)$ and $\phi_2(z)$ are the modal functions given by

$$\begin{aligned} &(\rho_0 W_i^2 \phi_{iz})_z + \rho_0 N^2 \phi_i = 0\,, \quad i = 1, 2 \\ &\phi_i = 0 \quad \text{at} \quad z = -h\,, \quad \text{and} \quad W_i^2\phi_{iz} = g\phi_i \quad \text{at} \quad z = 0. \end{aligned}$$

Here $W_i = c_i - u_0(z)$ where c_i is the long wave speed corresponding to the mode $\phi_i(z)$.

Derivation of coupled Ostrovsky equations

We are concerned with the case when there are two modes with nearly coincident speeds $c_1 = c$ and $c_2 = c + \alpha^2\Delta$, where Δ is the detuning parameter.
The asymptotic expansion then yields, at the next order, to the problem

$$\begin{aligned}
&\{\rho_0(c-u_0)^2\zeta_{2\theta z}\}_z + \rho_0 N^2\zeta_{2\theta} = M_2 \quad \text{at} \quad -h < z < 0,\\
&\rho_0(c-u_0)^2\zeta_{2\theta z} - \rho_0 g\zeta_{2\theta} = N_2 \quad \text{at} \quad z = 0\,,\\
&\zeta_2 = 0 \quad \text{at} \quad z = -h\,,
\end{aligned}$$

where M_2, N_2 are known expressions containing terms in A_i and their derivatives. Two compatibility conditions need to be imposed on this system, given by

$$\int_{-h}^{0} M_2\phi_{1,2}\,dz - [N_2\phi_{1,2}](z=0) = 0\,.$$

Derivation of coupled Ostrovsky equations

The outcome is the coupled Ostrovsky equations

$$I_1(A_{1\tau} + \mu_1 A_1 A_{1s} + \lambda_1 A_{1sss} - \gamma_1 B_1) + \nu_1 [A_1 A_2]_s$$
$$+\nu_2 A_2 A_{2s} + \lambda_{12} A_{2sss} = \gamma_{12} B_2 \,,$$

$$I_2(A_{2\tau} + \mu_2 A_2 A_{2s} + \lambda_2 A_{2sss} + \Delta A_{2s} - \gamma_2 B_2) + \nu_2 [A_1 A_2]_s$$
$$+\nu_1 A_1 A_{1s} + \lambda_{21} A_{1sss} = \gamma_{21} B_1 \,,$$

where $B_{1s} = A_1, B_{2s} = A_2$, and the coefficients are given by

$$I_i \mu_i = 3 \int_{-h}^{0} \rho_0 (c - u_0)^2 {\phi_i}_z^3 \, dz \,, \quad I_i \lambda_i = \int_{-h}^{0} \rho_0 (c - u_0)^2 {\phi_i}^2 \, dz \,,$$

$$I_i = 2 \int_{-h}^{0} \rho_0 (c - u_0) {\phi_i}_z^2 \, dz \,, \quad \lambda_{12} = \lambda_{21} = \int_{-h}^{0} \rho_0 (c - u_0)^2 \phi_1 \phi_2 \, dz \,,$$

$$\nu_1 = 3 \int_{-h}^{0} \rho_0 (c - u_0)^2 \phi_{1z}^2 \phi_{2z} \, dz \,, \quad \nu_2 = 3 \int_{-h}^{0} \rho_0 (c - u_0)^2 \phi_{2z}^2 \phi_{1z} \, dz \,,$$

$$I_i \gamma_i = \tilde{f}^2 \int_{-h}^{0} \rho_0 \Phi_i \phi_{iz} \, dz \,, \quad \gamma_{ij} = \tilde{f}^2 \int_{-h}^{0} \rho_0 \Phi_i \phi_{jz} \, dz \,.$$

Here $i, j = 1, 2$ and $\rho_0 W \Phi_{1,2} = \rho_0 W \phi_{1z,2z} - (\rho_0 u_0)_z \phi_{1,2}$, $W = c - u_0(z)$. If there is no shear flow, that is $u_0 = 0$, then $\gamma_1 = \gamma_2 = \tilde{f}^2 / 2c$ and $\gamma_{12} = \gamma_{21} = 0$.

Three-layer model with shear flow

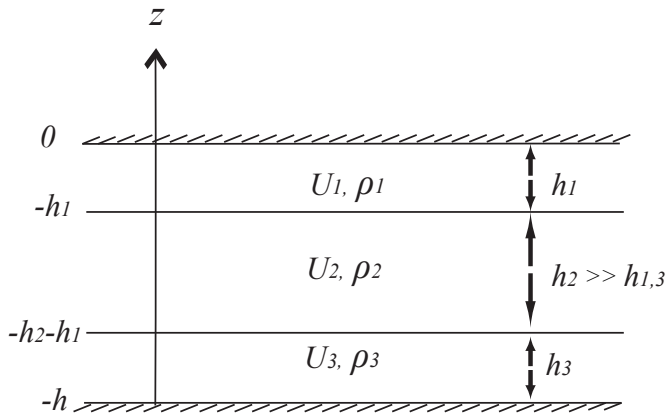

We assume $U_2 = 0$ without loss of generality. A resonance with two distinct modes can take place if

$$h_2 \gg h_1, h_3\,, \quad c = U_1 + \{\frac{g h_1(\rho_2 - \rho_1)}{\rho_1}\}^{1/2} = U_3 + \{\frac{g h_3(\rho_3 - \rho_2)}{\rho_3}\}^{1/2}\,.$$

For given densities $\rho_{1,2,3}$ and layer depths $h_{1,3}$, these determine the allowed shear $U_1 - U_3$. The modal functions and their derivatives are then found explicitly, and all coefficients of the scaled cO equations

$$(u_T + uu_X + u_{XXX} + n(uv)_X + mvv_X + \alpha v_{XXX})_X = \beta u + \gamma v,$$
$$(v_T + vv_X + \delta v_{XXX} + \Delta v_X + p(uv)_X + quu_X + \lambda u_{XXX})_X = \mu v + \nu u$$

are calculated.

Linear dispersion relation (without shear flow)

The structure of the linear dispersion relation determines the possible solution types.

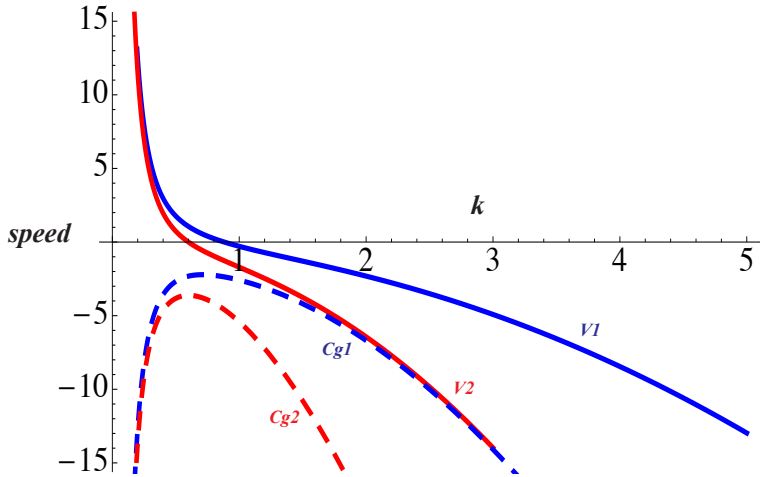

Figure: Dispersion curve in the absence of a shear flow ($\beta = \mu > 0$). The solid curves show the phase speed, and the dashed curves show the group velocity.

In the presence of a shear flow, $\beta \neq \mu$, and each can be either positive or negative.

Numerical simulations

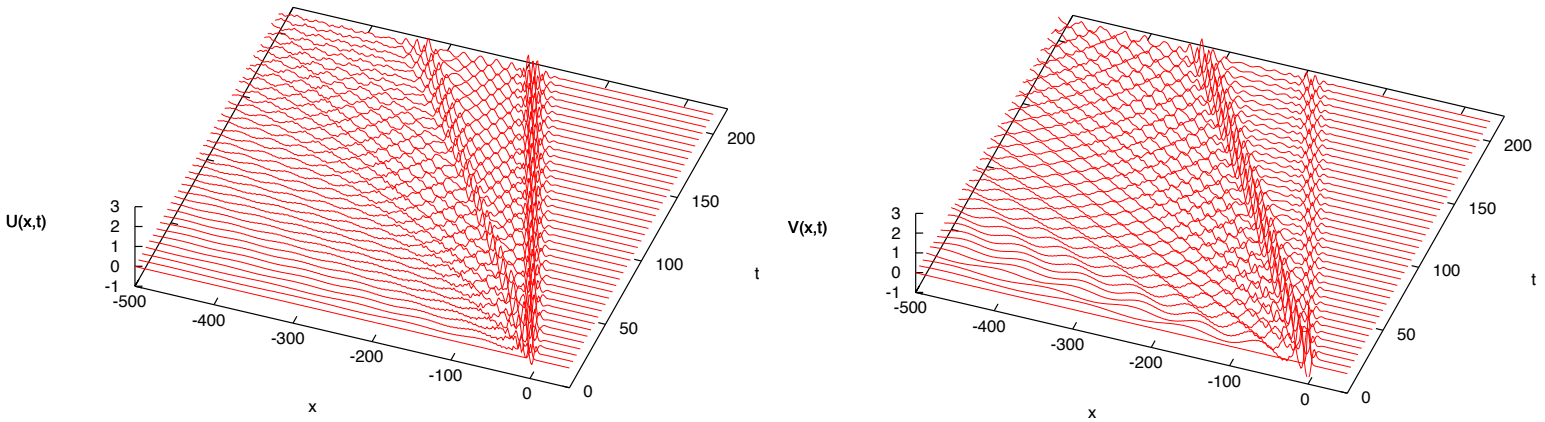

Figure: Typical numerical simulations for the coupled Ostrovsky equations without shear flow.

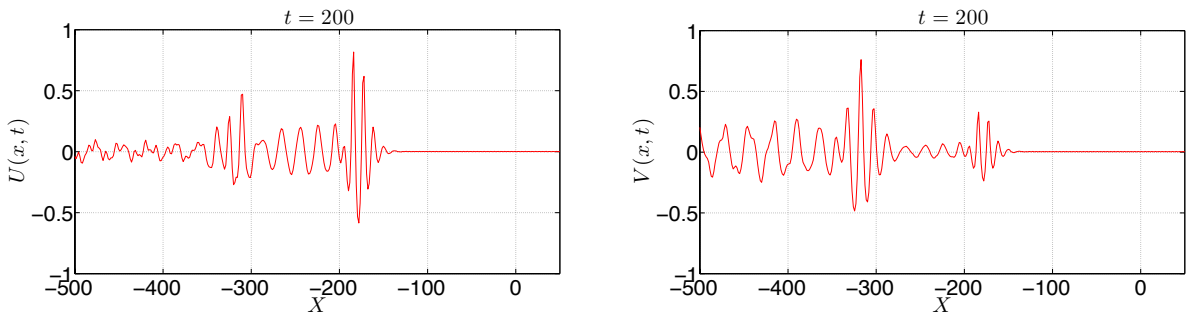

Figure: A cross-section at $t = 200$.

Linear dispersion relation (with a shear flow)

Case A ($\beta > 0, \mu > 0$): There is no spectral gap in either mode, and this case is similar to the situation without any background shear. For both modes the group velocities are negative for all k, and each has a turning point at $k = k_{m1,m2}$ respectively.

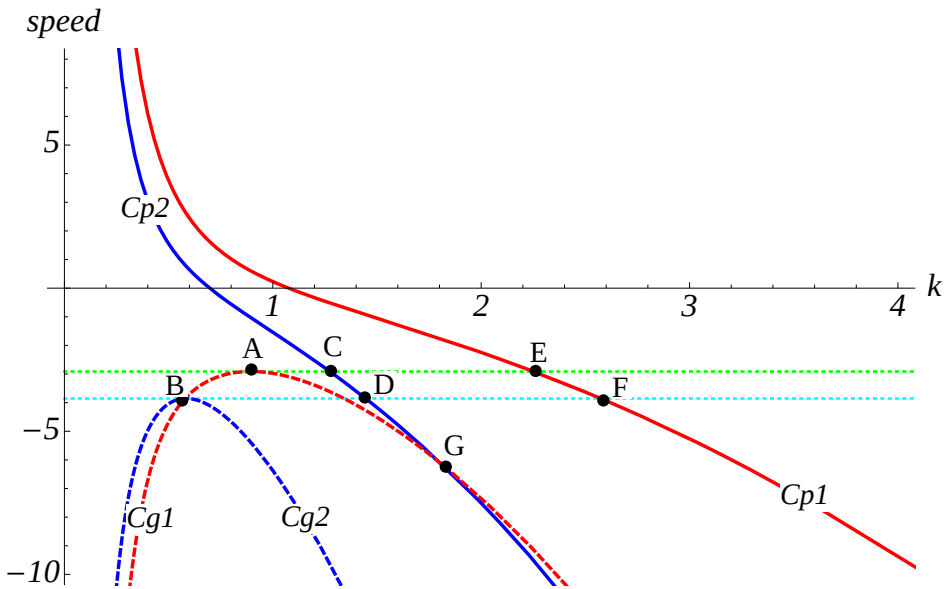

Figure: Typical dispersion curve for Case A.

Numerical simulations

Case A ($\beta > 0, \mu > 0$):

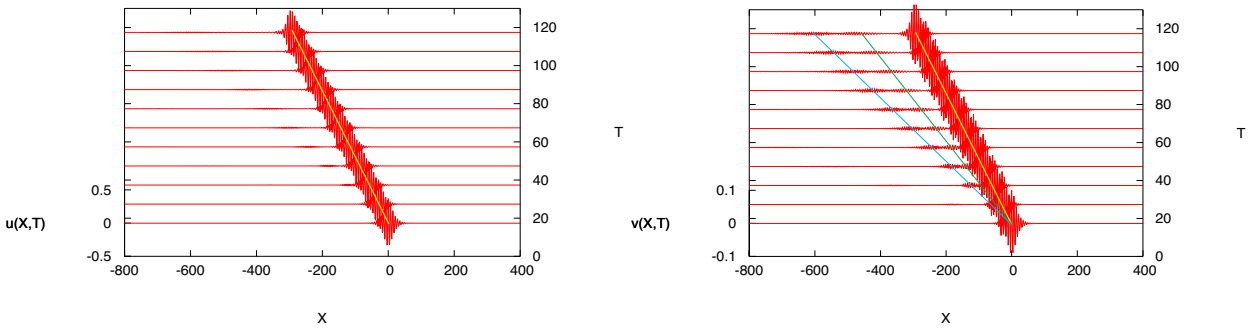

Figure: Numerical simulations (Case A) using the wave packet initial condition corresponding to the point A.

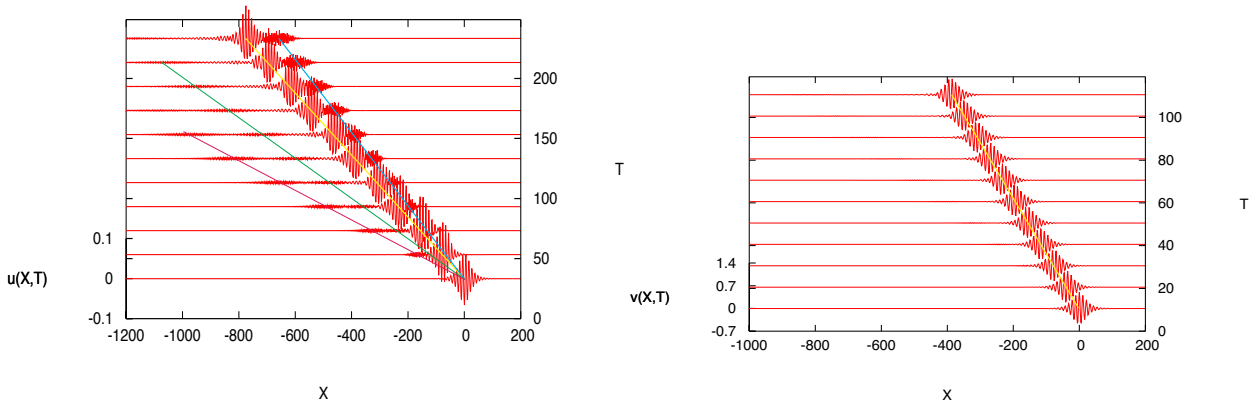

Figure: Numerical simulations (Case A) using the wave packet initial condition corresponding to the point B.

Numerical simulations

Case A ($\beta > 0, \mu > 0$):
A typical numerical result is shown below using the KdV solitary wave initial condition. The generation of two wave packets can be seen in the u-component, but one of them is too small to be seen in the v-component. However, the comparison of the numerical modal ratio, $R = u_0/v_0$, and the speeds of the wave packets, shows a very good agreement with the theoretical predictions from the dispersion relation.

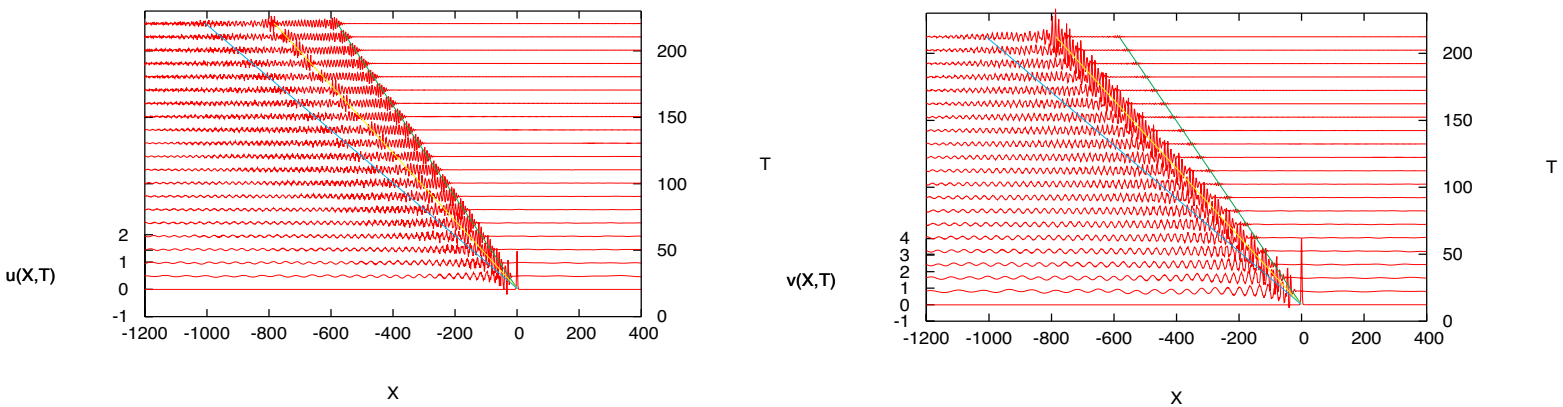

Figure: Numerical simulations (Case A) using the weak coupling KdV initial condition.

Linear dispersion relation (with a shear flow)

Case B ($\beta > 0, \mu < 0$): There is no spectral gap in mode 1, and the group velocity is negative for all k with a turning point at $k = k_{m1}$. But mode 2 has a spectral gap, as the phase speed has a maximum value, c_{s2} at $k = k_{s2}$. The group velocity is positive as $k \to 0$ and negative as $k \to \infty$. At the value $c_{p2} = c_{s2}$, the phase and group velocities are equal.

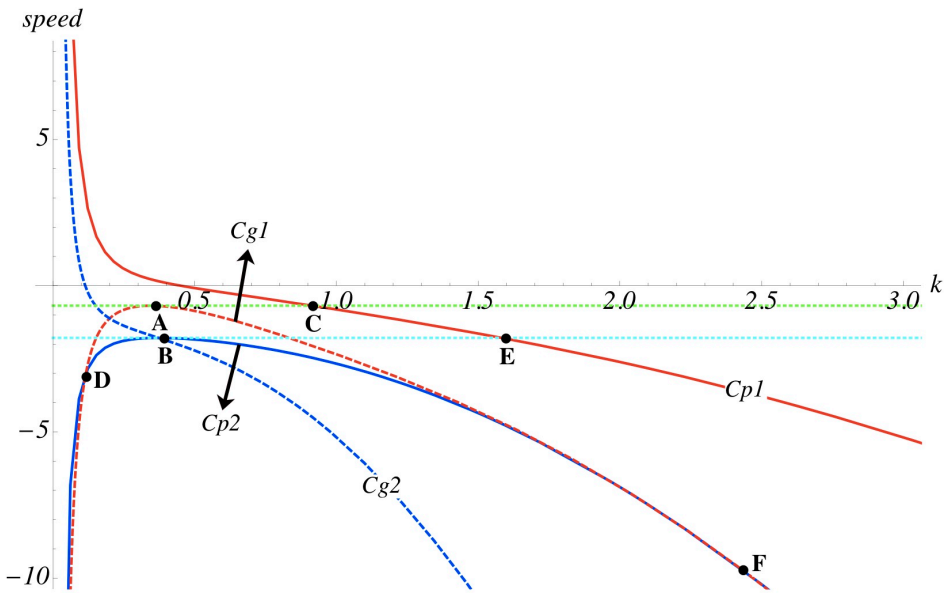

Figure: Typical dispersion curve for Case B.

Numerical simulations

Case B ($\beta > 0, \mu < 0$):

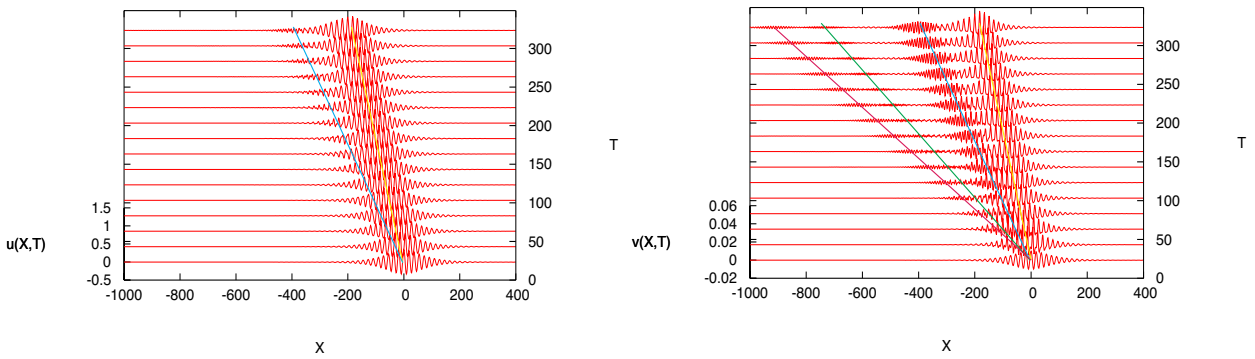

Figure: Numerical simulations for Case B using the wave packet initial condition corresponding to the point A.

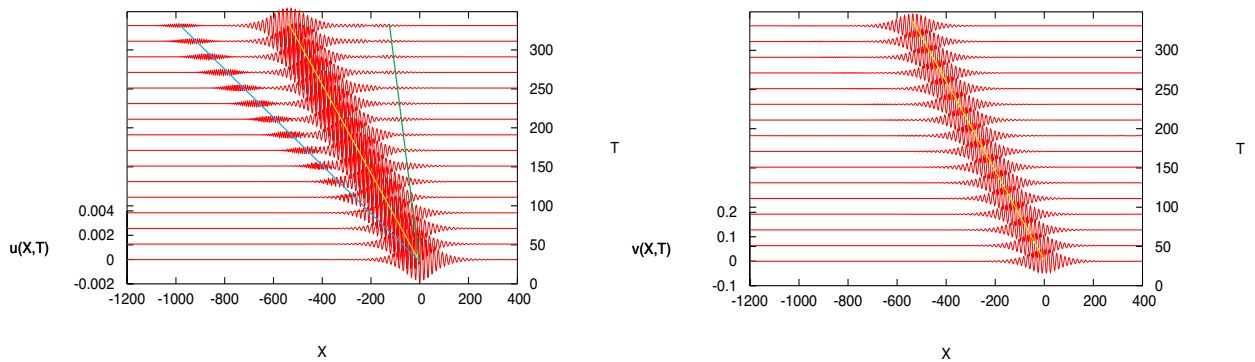

Figure: Numerical simulations for Case B using the wave packet initial condition corresponding to the point B.

Numerical simulations

Case B ($\beta > 0, \mu < 0$):

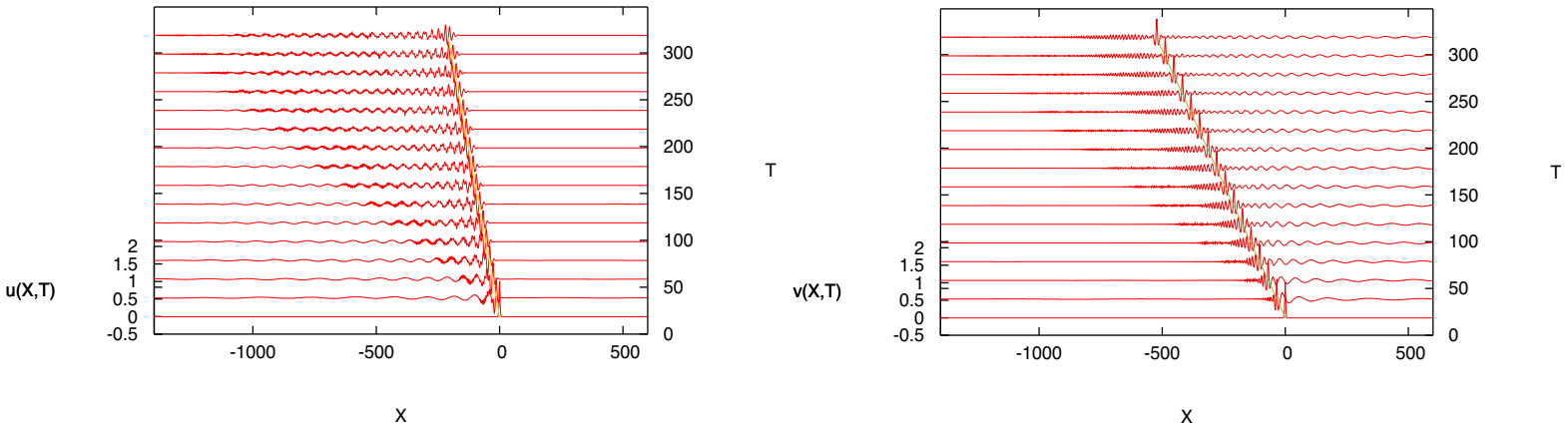

Figure: Numerical simulations for Case B using the KdV weak coupling initial condition.

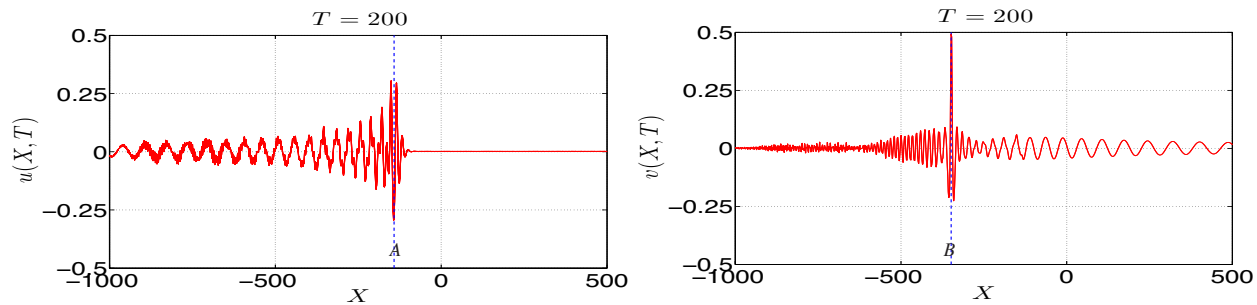

Figure: A cross-section at $T = 200$ for both modes.

Linear dispersion relation (with a shear flow)

Case C ($\beta < 0, \mu > 0$): There is no spectral gap in mode 1, and the group velocity is negative for all k with a turning point at $k = k_{m1}$. But mode 2 has a spectral gap, as the phase speed has a maximum value, c_{s2} at $k = k_{s2}$.The group velocity is positive as $k \to 0$ and negative as $k \to \infty$. At the value $c_{p2} = c_{s2}$, the phase and group velocities are equal. There are two maxima in c_{g1}.

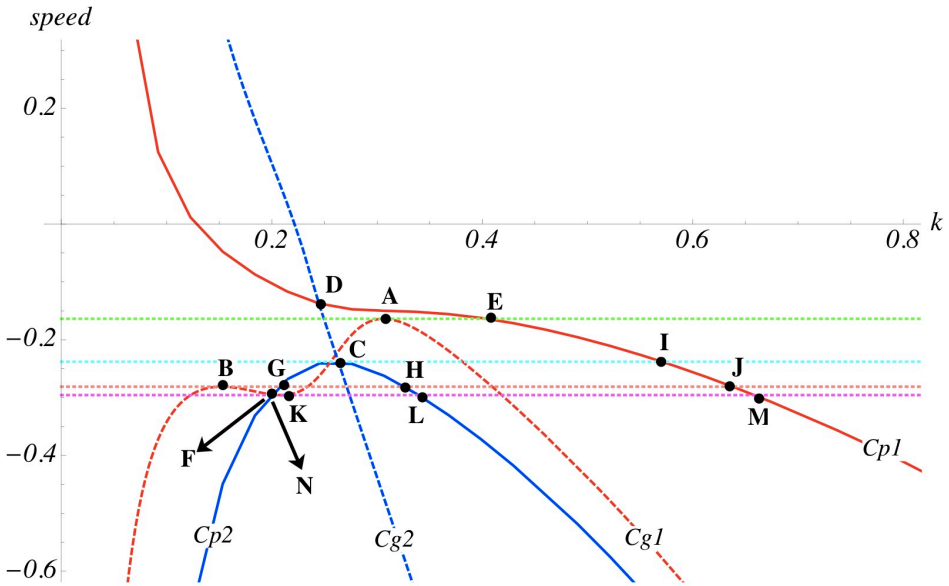

Figure: Typical dispersion curve for Case C.

Numerical simulations

Case C ($\beta < 0, \mu > 0$):

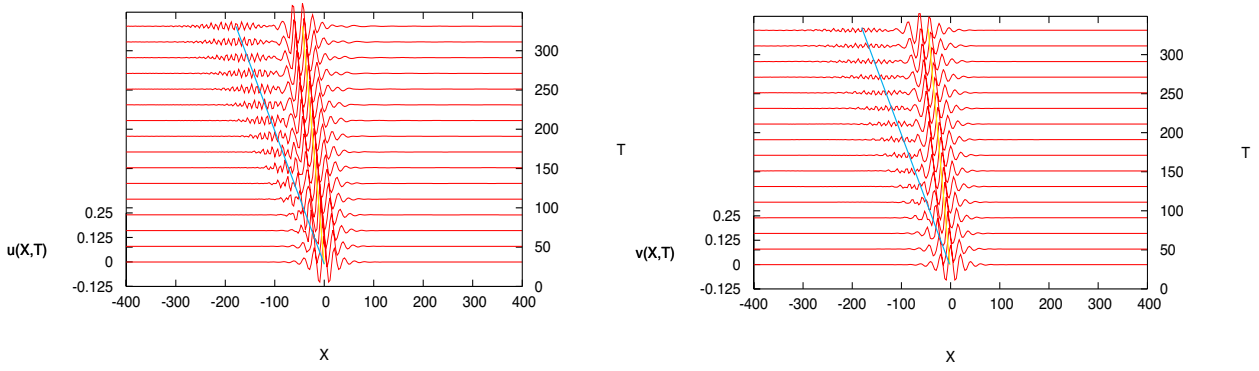

Figure: Numerical simulations for Case C using the wave packet initial condition corresponding to the point A.

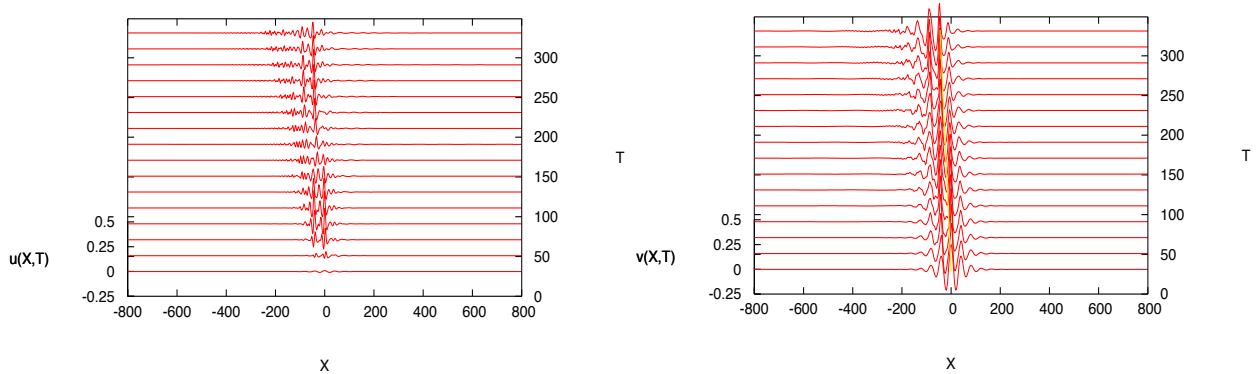

Figure: Numerical simulations for Case C using the wave packet initial condition corresponding to the point B.

Numerical simulations

Case C ($\beta < 0, \mu > 0$):

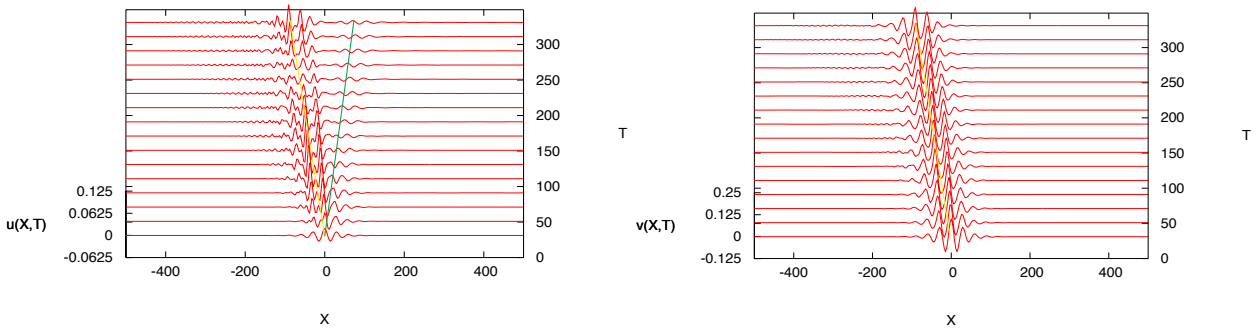

Figure: Numerical simulations for Case C using the wave packet initial condition corresponding to the point K.

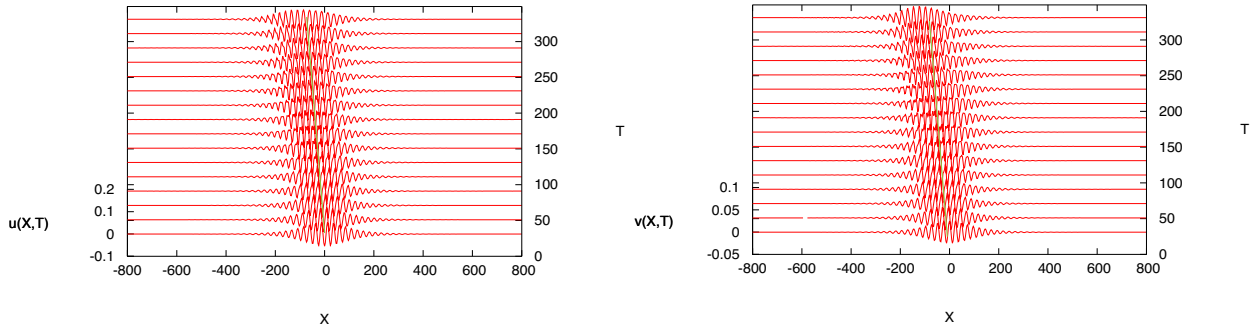

Figure: Numerical simulations for Case C using the wave packet initial condition corresponding to the point C.

Numerical simulations

Case C ($\beta < 0, \mu > 0$):

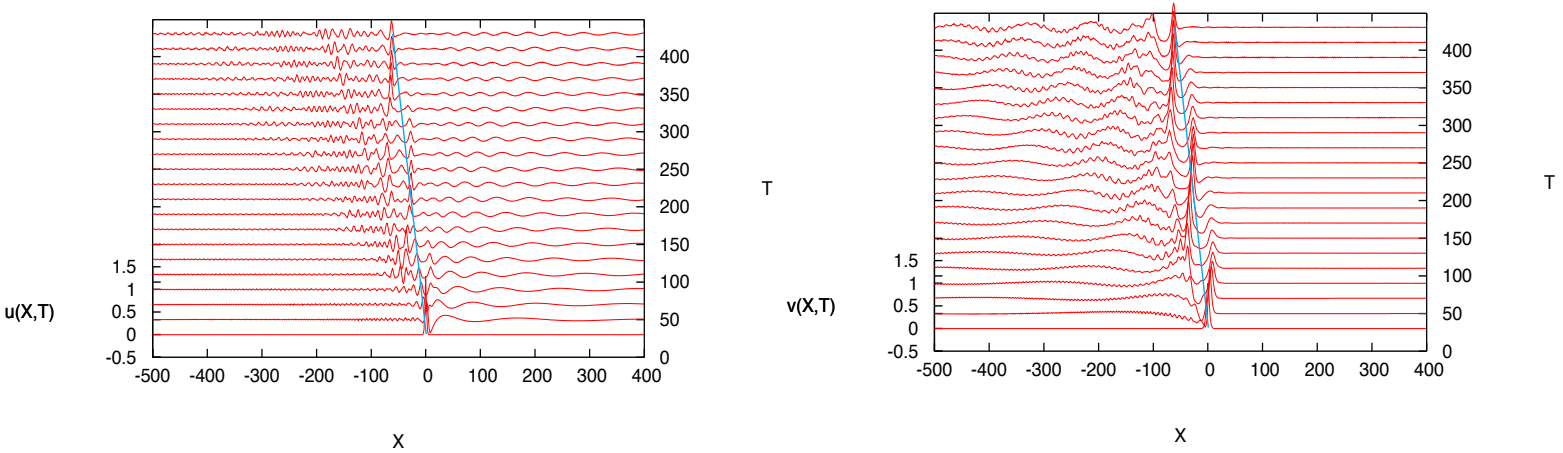

Figure: Numerical simulations for Case C using the KdV weak coupling initial condition.

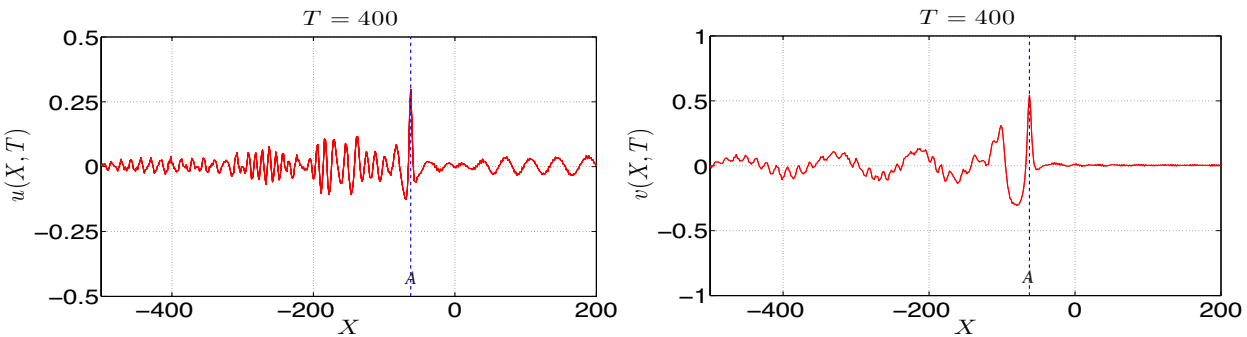

Figure: A cross-section at $T = 400$ for both modes.

Linear dispersion relation (with a shear flow)

Case D ($\beta < 0, \mu < 0$): Now both modes have phase speeds with maxima c_{s1}, c_{s2} at $k = k_{s1}, k_{s2}$ respectively. For both modes, the group velocity is positive as $k \to 0$, but negative as $k \to \infty$, and at the point of maximum phase speed, the phase and group velocities for each mode are equal.

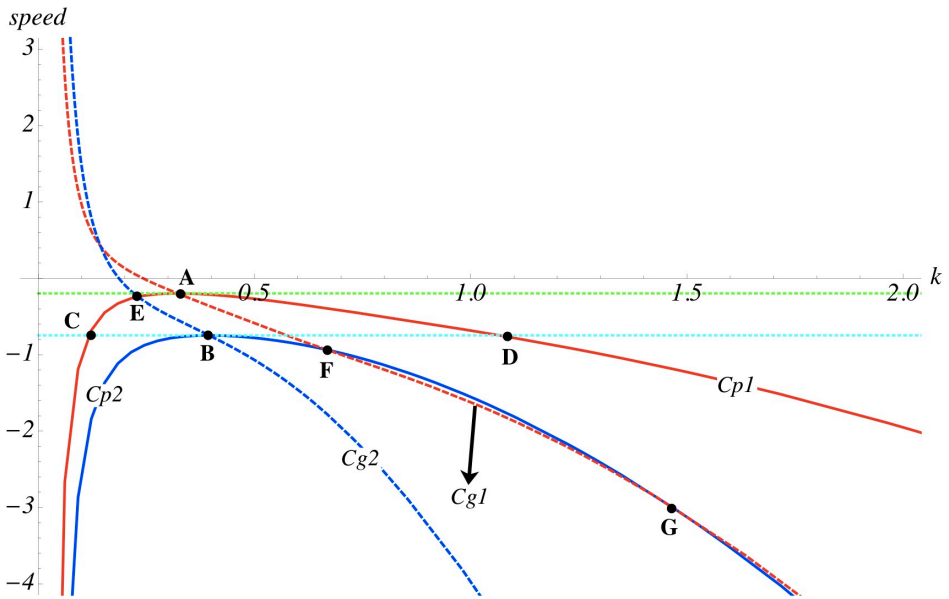

Figure: Typical dispersion curve for Case D.

Numerical simulations

Case D ($\beta < 0, \mu < 0$) :

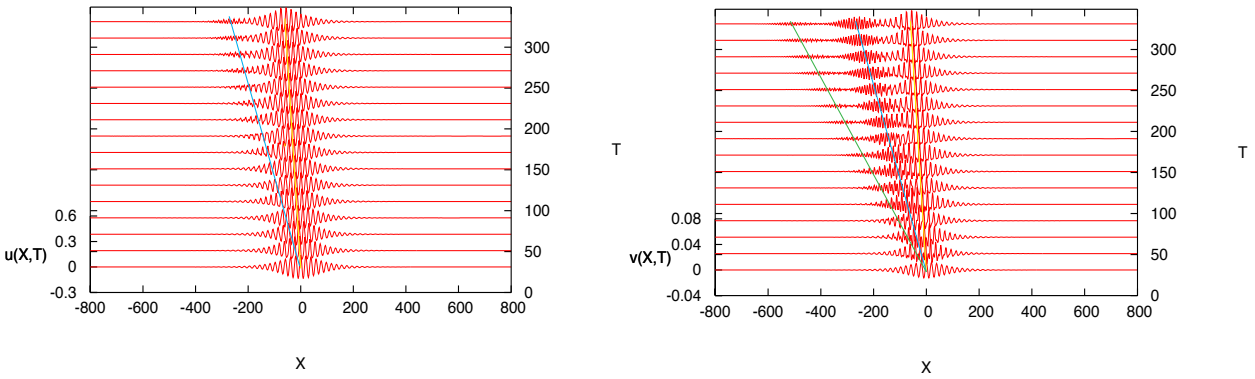

Figure: Numerical simulations for Case D using the wave packet initial condition corresponding to the point A.

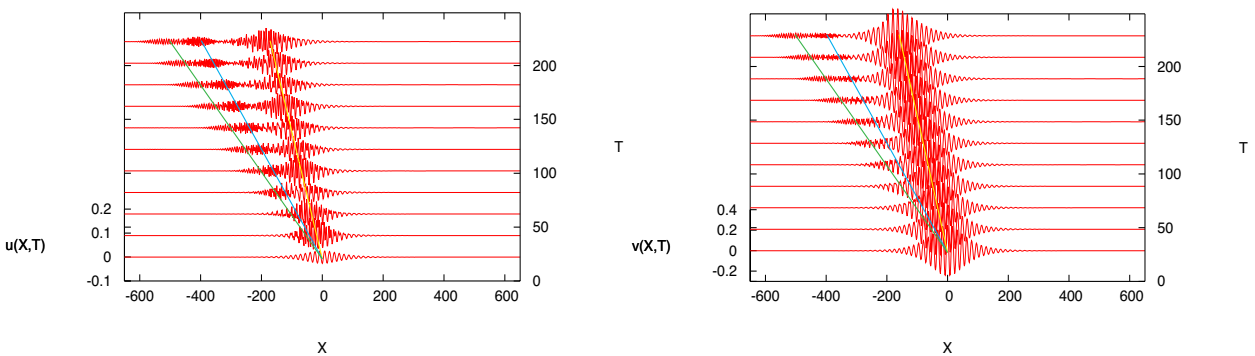

Figure: Numerical simulations for Case D using a wave packet initial condition corresponding to point B.

Numerical simulations

Case D ($\beta < 0, \mu < 0$):

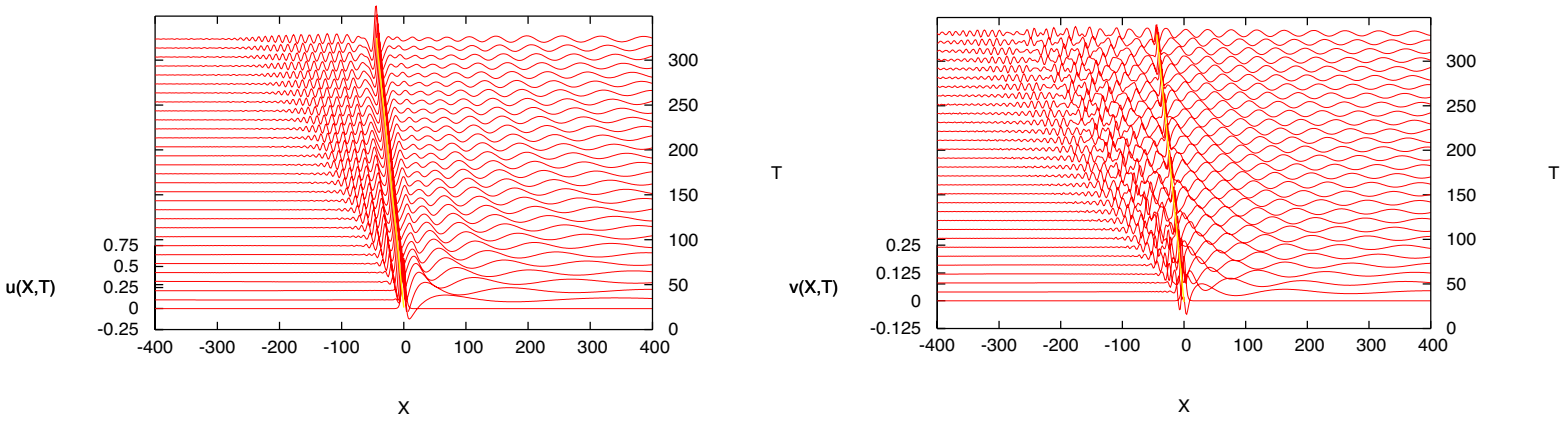

Figure: Numerical simulations for Case D using the KdV weak coupling initial condition.

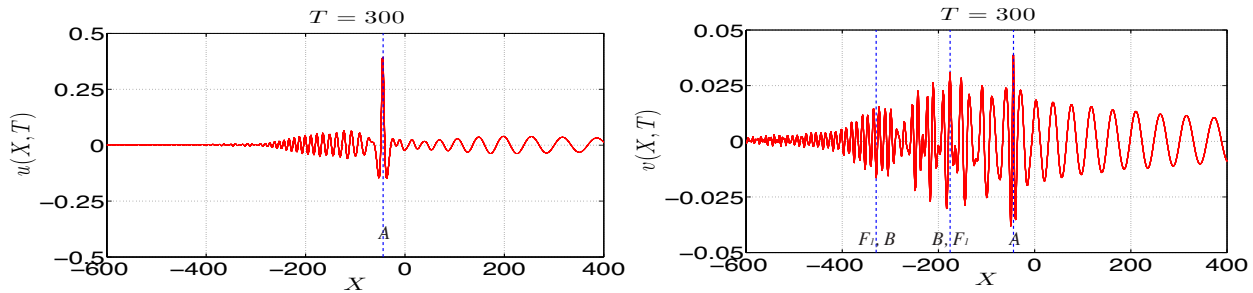

Figure: A cross-section at $T = 300$ for both modes.

Concluding remarks

- Coupled Ostrovsky equations are derived for strongly interacting internal waves in a density-stratified ocean with a shear flow.
- In the absence of a shear flow, initial solitary-like waves are destroyed and replaced by two coupled unsteady nonlinear wave packets, being the counterpart of the same phenomenon in the single Ostrovsky equation.
- There are several typical solution types when there is a shear flow. Dominant features of the observed dynamical behaviours can be classified and interpreted in terms of the main features of the relevant dispersion curves.
- Sufficiently strong current near a pycnocline may lead to situations where $\lambda\gamma < 0$ for a single Ostrovsky equation (anomalous case).

Main references

1. L. Ostrovsky, Oceanogology 18 (1978) 119-125.
2. J. Gear and R. Grimshaw, Stud. Appl. Math. 70 (1984) 235-258.
3. R. Grimshaw, Stud. Appl. Math. 73 (1985) 1-33.
4. R. Grimshaw, L.A. Ostrovsky, V.I. Shrira, V. I. and Y.A. Stepanyants, Surveys Geophysics 19 (1998) 289-338.
5. M.A. Obregon and Yu.A. Stepanyants, Phys. Lett. A 249 (1998) 315-323.
6. K.R. Helfrich, Phys. Fluids 19 (2007) 026601.
7. R.H.J. Grimshaw and K.R. Helfrich, Stud. Appl. Math. 121 (2008) 71-88.
8. R.H.J. Grimshaw, K.R. Helfrich, and E.R. Johnson, Phys. Fluids, 25 (2013) 056602.
9. A. Alias, R.H.J. Grimshaw, K.R. Khusnutdinova, Chaos 23 (2013) 023121.
10. A. Alias, R.H.J. Grimshaw, K.R. Khusnutdinova, arXiv: 1407.0939v1 [nlin.PS] 3 Jul 2014.